Available online at www.sciencedirect.com
SCIENCE DIRECT®

Journal of the European Ceramic Society 23 (2003) 2677–2682
www.elsevier.com/locate/jeurceramsoc

Structural study of $Ca_{0.7}Nd_{0.3}Ti_{0.7}Al_{0.3}O_3$ dielectric ceramics using synchrotron X-ray diffraction

E.R. Kipkoech[a,*], F. Azough[a], R. Freer[a], C. Leach[a], S.P. Thompson[b], C.C. Tang[b]

[a]*Manchester Materials Science Centre, The University of Manchester/UMIST, Manchester M1 7HS, UK*
[b]*Daresbury Laboratory, Warrington, Cheshire WA4 4AD, UK*

Abstract

The crystal structure of $Ca_{0.7}Nd_{0.3}Ti_{0.7}Al_{0.3}O_3$ has been determined using synchrotron X-ray diffraction. Data were collected from a polycrystalline sample for Rietveld analysis. At room temperature, the structure exhibits an octahedral tilted framework (perovskite-type) with an orthorhombic lattice ($a=5.3803$ Å, $b=5.4003$ Å and $c=7.6140$ Å). The positions of the atoms in the unit cell and their isotropic temperature factors have been determined, together with the occupations of sites by Ca/Nd and Al/Ti atoms. The structure was determined to feature an $a^-a^-c^+$ orthorhombic tilt system in association with displacement of the A-site cations.

Keywords: Dielectric properties; Perovskites; X-ray methods; Synchotron radiation; $(Ca,Nd)(Ti,Al)O_3$

1. Introduction

A number of new materials have been developed for the expanding telecommunications market in the past decade. These applications require a combination of high relative permittivity (ε_r), to enable size reduction of devices, low dielectric loss in the high frequency region, (i.e. high quality factor, Q_f) to ensure spectral purity at microwave frequencies and near zero temperature coefficient of resonant frequency (τ_f) to ensure high stability of devices.[1] Several dielectric materials have been developed that meet these requirements in different frequency ranges. The existing dielectric materials can be classified according to their relative permittivities. High permittivity materials (ε_r typically 90–130) include ceramics based on $BaO–Nd_2O_3–TiO_3$[2] and $CaO–Li_2O–Ln_2O_3–TiO_2$;[3] medium permittivity (ε_r ~40–60) based on $CaO–TiO_2–Nd_2O_3–Al_2O_3$[4] (so called CTNA) and $ZrO_2–TiO_2–ZnO–Nb_2O_5$;[5] and finally low permittivity (ε_r ~20–40) dielectrics include $BaO–ZnO–Ta_2O_5$ and related complex perovskites.[1]

Ceramic materials with the perovskite-type structure dominate the low and medium permittivity range of microwave dielectric ceramics, providing the highest quality factor, temperature-stable dielectric ceramics. Moreover, the versatility of the perovskite structure provides the possibility of making solid solutions designed to achieve specific requirements. The main factors considered when selecting candidate materials for solid solutions include the dielectric properties of the end members, compatibility of their crystal structures, tolerance factor and processing conditions. It is found that most microwave dielectric ceramics with a high dielectric constant have large positive τ_f values. However, compensation of τ_f can be achieved by combining two compatible compounds with τ_f of opposite polarity or by modifying the unit cell with selective substitution of cations. This has been extensively demonstrated using $CaTiO_3$ and $SrTiO_3$ ceramics, which have high relative permittivities of approximately 170 and 230, respectively, with large positive temperature coefficients of resonant frequencies of +859 and +1647 ppm/°C, respectively.[6] Temperature stable ceramics have been effectively fabricated by combining $CaTiO_3$ or $SrTiO_3$ with $REAlO_3$,[4,7,8] $REGaO_3$,[8,9] $Ca/Sr(B^{2+/3+}B^{5+})O_3$[10–11] and $RE(B^{2+}B^{4+/6+})O_3$,[12–15] where RE = Rare Earth. In particular, solid solutions of $xCaTiO_3–(1-x)NdAlO_3$ (CTNA) form an important system and exhibit low temperature coefficient (τ_f ~0 ppm/°C), medium range relative permittivity (ε_r ~45) and high Q value (> 43,000 GHz), at $x=0.7$.[4,7,8]

$CaTiO_3$ has a distorted perovskite structure with orthorhombic symmetry at room temperature.[16] It is structurally compatible with $NdAlO_3$, which has a similar perovskite-type structure with rhombohedral

* Corresponding author.

0955-2219/03/$ - see front matter
doi:10.1016/S0955-2219(03)00148-1

symmetry at room temperature.[17] $NdAlO_3$ has a negative τ_f of ≈ -33 ppm/°C, relative permittivity of ≈22.3 and high Q value ($Q_f = 58{,}000$ GHz).[17] Jancar et al.[4] and Kim et al.[7] reported that $CaTiO_3$ and $NdAlO_3$ form solid solutions over the composition range $x CaTiO_3$-$(1-x)NdAlO_3$ ceramics, where $x = 0$–1. Although the general features of the crystal lattice in the solid solution are known,[4,7] the structural details have not previously been examined. We have therefore undertaken synchrotron radiation studies to gain insight into the detailed structure of a commercially important CTNA ceramic. Recently, it has been successfully demonstrated that synchrotron radiation is a viable technique for detailed structural studies of complex high permittivity microwave dielectric ceramics.[18]

2. Experimental

A large cylindrical commercially prepared $CaTiO_3$–$NdAlO_3$ ceramic sample (of nominal composition $Ca_{0.7}Nd_{0.3}Ti_{0.7}Al_{0.3}O_3$) 30 mm diameter and 15 mm thickness was used for the investigation. The dielectric properties were first determined using the Hakki-Coleman technique; the measurement frequency was 2.895 GHz. Elemental analysis was performed on samples (polished to mirror-like finish) using a CAMECA (SX 100, Paris, France), Electron Probe Microanalyser operating at 15 kV with 20 mA beam current. Synthetic corundum and synthetic rutile were used as calibration standards for Al and Ti, respectively. Natural wollastonite ($CaSiO_3$) was used for Ca, while synthetic rare earth glass, containing Nd^{3+}, was used as standard for Nd. The chemical composition was determined from the average of analyses performed at six different locations on the sample. Additional energy-dispersive (EDS) system analyses were undertaken using a Philips 525 Scanning Electron Microscope. Detailed X-ray diffraction measurements were performed on Station 2.3 at the synchrotron radiation source of Daresbury Laboratory. The angular-dispersive instrument is purposely built for high-resolution powder diffraction to solve crystal structures in materials.[19] In the experiment, a 1.8 mm (vertical) × 10 mm (horizontal) X-ray beam of $\lambda = 1.4$ Å was used to achieve a large illuminated sample area. The tuned wavelength was calibrated to be $\lambda = 1.40019(5)$ Å using a high quality silicon powder (NIST 640B standard). The figure in the parentheses is the estimated standard deviations (e.s.d).[20] The calibrated beam was incident onto the flat surface of the sample. A total of 4 repeat scans of $\theta/2\theta$ geometry from 20 to 110° 2θ with a step 0.01° and 1 s per point, were collected. These scans were summed to give a single pattern to improve the statistics and the background was subtracted. The pattern was analysed by the Rietveld method[21] to extract crystallographic information as used in previous work.[18]

3. Results and discussion

The relative permittivity of the commercial CTNA sample was determined to be 46.2 ± 0.5 and the Q_f value was $40{,}400 \pm 1000$ GHz. The relative permittivity is comparable with published data[4,7,8] but the Q-values are slightly lower than published data because of differences in measurement techniques. A typical SEM micrograph of the CTNA ceramic specimen is shown in Fig. 1. The specimen exhibits a variable grain size with grains in the range 5–12 μm. There is evidence of a minor second phase, characterised by elongated grains approximately 1.0 μm long and less than 0.5 μm wide. The second phase is rich in alumina as indicated by the EDS spectra (Fig. 2). However, the second phase is too small to yield accurate quantitative compositional data. A similar, Al-rich, phase was observed by Kim et al.[7] in compositions with $x CaTiO_3$-$(1-x)NdAlO_3$, where $x = 0.7$–0.9. Compositional analysis of the matrix phase of the present ceramic is shown in Table 1. This yields a formula equivalent to $Ca_{0.713}Nd_{0.312}Ti_{0.703}Al_{0.275}O_{2.998}$.

Experimental X-ray diffraction data and the results of the final least squares refinement are presented in Fig. 3.

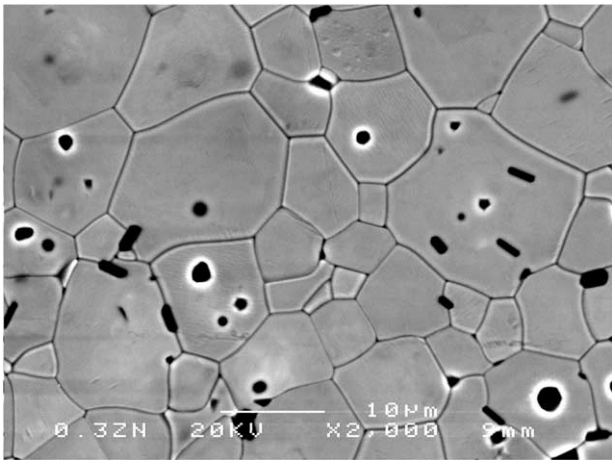

Fig. 1. Typical SEM micrograph of the $Ca_{0.7}Nd_{0.3}Al_{0.3}Ti_{0.7}O_3$ sample.

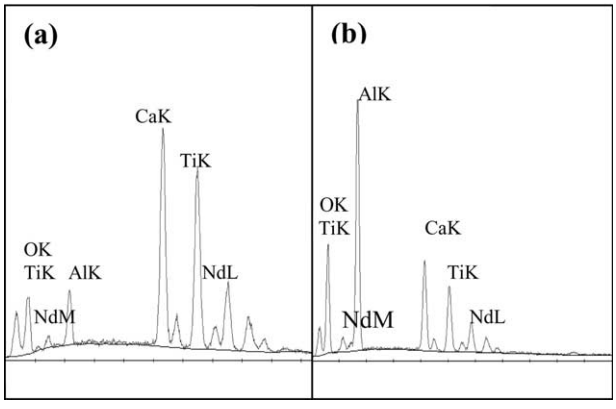

Fig. 2. Energy dispersive spectra for (a) matrix phase and (b) minor phase typified by small dark elongated grains.

Table 1
Elemental composition of commercial ceramic sample

Element	At.%
Nd	6.23
Ca	14.26
Ti	14.05
Al	5.50
O	59.96
Total	100.0

Table 2
Instrumental parameters and crystallographic information

Wavelength, λ	1.40019(5) Å
2θ-zero point	−0.0014(2)°
Peak function parameters (pseudo-Voigt)	$U=232.3$, $V=112.5$, $W=-1.34$
Peak mixing parameter	0.433
2θ range	20–110°
Number of reflections	199
Number of refined parameters	19
Space group	Pbnm (No. 62), $Z=4$
Lattice parameters (Å)	$a=5.3803(1)$, $b=5.4003(1)$, $c=7.6140(1)$, $\alpha=\beta=\lambda=90°$
R-factors	$R_I=3.50\%$, $R_{WP}=8.65\%$, $R_{EXP}=7.63\%$

The XRD spectrum (Fig. 3) was initially indexed for an orthorhombic system. Constrained by symmetry operators of *Pbnm* (No. 62), the instrumental parameters and crystallographic information (Table 2) were obtained from the final Rietveld refinement. The modelled structures in Figs. 4 and 5 are good representations as demonstrated by the excellent fit to the experimental data (Fig. 3). The accuracy of fit is also indicated by the agreement in the *R*-factors, where the weighed value ($R_{WP}=8.65\%$) is close to the expected value ($R_{EXP}=7.63\%$) (Table 2).

Initial refinements of the atom site occupations yielded acceptable results, but the overall improvement was very small ($R_{WP}=8.46\%$). The octahedral centres (Fig. 4) are occupied by ~60% Ti atoms sharing with ~40% Al atoms. The larger cations (Ca and Nd) represented by spheres in Fig. 4 are distributed in the rhombic cavity channelling along the c-axis. These sites are occupied in the ratio 70:30% for Ca:Nd. However, the final refinement presented here was carried out with the occupations fixed at $Ca^{2+}=70\%$, $Nd^{3+}=30\%$, $Ti^{4+}=70\%$ and $Al^{3+}=30\%$, which matches well the values determined by chemical analysis.

The atomic co-ordinates and temperature factors given in Table 3 are consistent with those of $GdFeO_3$-type orthorhombic perovskites.[16] The distortion from the ideal cubic perovskite may be described as tilting of the oxygen octahedra surrounding the Al/Ti atoms. In

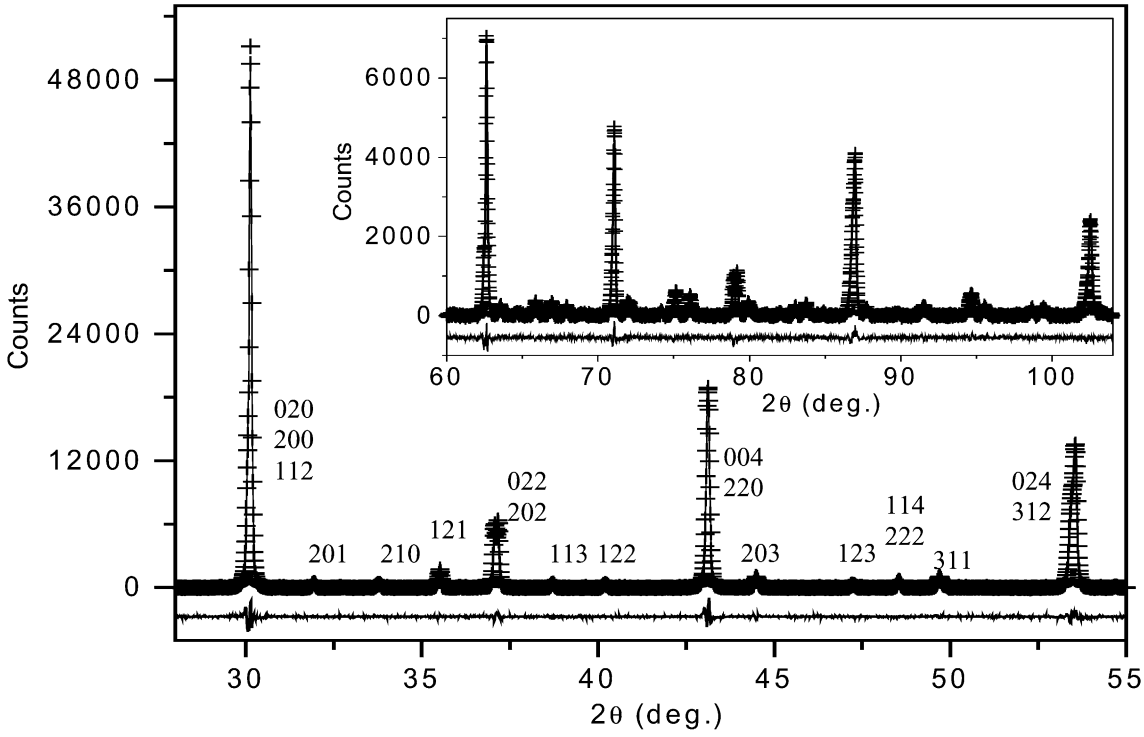

Fig. 3. XRD spectrum and refinement of the $Ca_{0.7}Nd_{0.3}Al_{0.3}Ti_{0.7}O_3$ sample. The experimental data are shown as crosses, fitted results as solid line and difference as solid line below the main data. For presentation purposes, data below $2\theta=28°$ are not shown. Data for $2\theta=28$–$55°$ are indexed where the assignment is unambiguous.

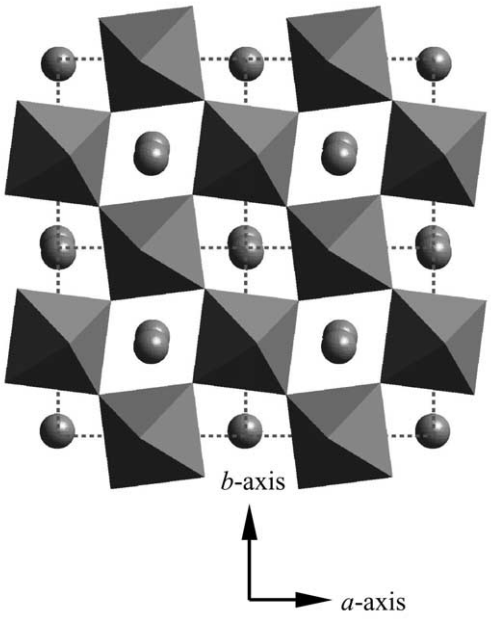

Fig. 4. The structure of $Ca_{0.7}Nd_{0.3}Al_{0.3}Ti_{0.7}O_3$ showing four unit cells, viewed along the *c*-axis with the *a*- (horizontal) and *b*-axis (vertical). The octahedra represent Al/TiO_6 molecules and the spheres are either Ca or Nd cations.

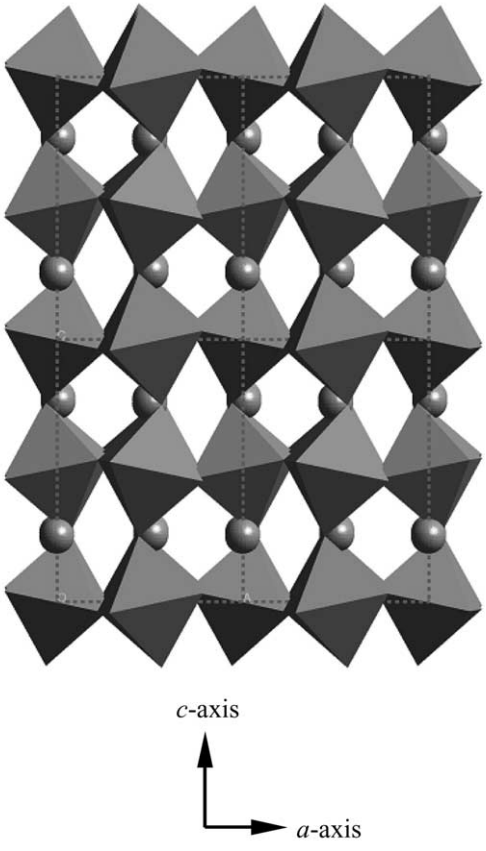

Fig. 5. The structure of $Ca_{0.7}Nd_{0.3}Al_{0.3}Ti_{0.7}O_3$ showing four unit cells, viewed along the *b*-axis with the *a*-axis horizontal and *c*-axis vertical. The octahedra and spheres have the same representation as in Fig. 4.

Table 3
Fractional atom positions, isotropic thermal parameters (*B*)

Atom	*x*	*y*	*z*	B (Å^2)
Ca	−0.0033(4)	0.0251(1)	0.25	0.55(1)
Nd	−0.0033(4)	0.0251(1)	0.25	0.55(1)
Al	0.00000	0.50000	0	0.45(2)
Ti	0.00000	0.50000	0	0.45(2)
O1	0.0629(8)	0.4894(5)	0.25	0.26(3)
O2	0.7180(6)	0.2821(5)	0.0369(4)	0.26(3)

Fig. 3, both odd–odd–odd and odd–odd–even reflections are present illustrating that the oxygen octahedra are tilted both in-phase and anti-phase, respectively. The octahedral rotations occur about the inversion centres at the Al/Ti atoms and rotate the $(Al/Ti)O_6$ units as rigid bodies. In the notation of Glazer[22] the tilt mechanism can be described by a simple three tilt system denoted as $a^-a^-c^+$. The c^+ tilt indicates that $(Al/Ti)O_6$ octahedra rotate about the [001] axis of the pseudocubic cell by an angle *c*. The magnitude of rotation along this axis is preserved by mirror planes perpendicular to the rotation axis. Thus all successive octahedra linked along this axis are rotated in the same direction denoted by + superscript on c^+ as projected in Fig. 4. The single tilt about the a-axis is decomposed into two tilts of equal magnitude with respect to [100] and [010] axes of the pseudo-cubic cell, represented as a^-a^-. The negative superscript on the [100] and [010] axis tilts indicate that successive octahedra along these axes rotate in anti-phase, that is, a^+ and a^- sequentially (Fig. 5). In this tilting mechanism the A-site cations are displaced from their ideal location in prototypic perovskites with a resultant loss of the A-site inversion centres. In contrast, the original cubic symmetry persists in approximate form near each B-site thus retaining the inversion centres throughout the lattice.

In Tables 4 and 5 the interatomic distances are presented where the atoms are numbered in accordance with Sasaki et al.[15] The six-fold coordination is maintained for the B-sites at the centre of the near-perfect octahedra as indicated by the small variations in Al/Ti–O bond lengths, where the shortest A/Ti–O1 bond is 1.9342(8) Å and the longest Al/Ti–O2 bond is 1.943(3) Å. However, two of the Ca/Nd-O bonds are non-bonding (> 3.0 Å) thus reducing the coordination number of Ca/Nd atoms to 10 acentric bonds in contrast to 12 for ideal cubic perovskites. The geometry of the Ca/Nd coordination sphere defined by the tilted octahedra is therefore a distorted cuboctahedron (Fig. 4) in relation to the ideal A-site polyhedron in cubic perovskites which is that of a cuboctahedron composed of four triangular and six square faces.[23]

The deviation from the cubic perovskite (also denoted by the tolerance factors which is less than 1.0, $t_o = 0.9740$), can therefore be considered in terms of

Table 4
The interatomic distances in Al/Ti octahedra (left) and cub-octahedron (right) with e.s.d. in parentheses

Atom–atom	Distance (Å)
Ca/Nd(i)–O1(i)	2.377(5)
Ca/Nd (i)–O1(iv)	2.533(3)
Ca/Nd(i)–O1(iii)	3.017(5)
Ca/Nd(i)–O1(v)	2.914(3)
Ca/Nd(i)–O2(i')	2.385(3)
Ca/Nd(i)–O2(iv')	2.609(3)
Ca/Nd(i)–O2(v)	2.697(3)
Ca/Nd(i)–O2(viii)	3.143(3)
Al/Ti(i)–O1(i)	1.9342(8)
Al/Ti(i)–O2(v)	1.941(3)
Al/Ti(i)–O2(viii)	1.943(3)
O1(i)–O2(v)	2.772(5)
O1(i)–O2(iv)	2.723(4)
O1(i)–O2(i)	2.706(5)
O1(i)–O2(viii)	2.760(4)
O2(v)–O2(viii)	2.722(4)
O2(v)–O2(iv)	2.770(5)

Table 5
Metal-metal distances with standard deviations in parentheses

Metal–metal	Distance (Å)
Ca/Nd(i)–Al/Ti(i)	3.313(2)
Ca/Nd(i)–Al/Ti(iii)	3.4152(4)
Ca/Nd(i)–Al/Ti(v)	3.284(2)
Ca/Nd(i)–Al/Ti(vii)	3.1941(4)
Al/Ti(i)–Al/Ti(iii)	3.8115(2)
Al/Ti(i)–Al/Ti(ii)	3.8070(2)
Ca/Nd(i)–Ca/Nd(iii)	3.836(3)
Ca/Nd(i)–Ca/Nd(v)	3.787(3)
Ca/Nd(i)–Ca/Nd(ii)	3.8167(2)

rotation of the essentially rigid $(Al/Ti)O_6$ octahedra from their alignment within the ideal perovskite and the displacement of the A-site cations from the ideal perovskite location.

4. Conclusions

The structural details of a CTNA microwave dielectric ceramic of composition equivalent to $Ca_{0.713}Nd_{0.312}Ti_{0.703}Al_{0.275}O_{2.998}$ have been determined. Synchrotron XRD data were collected from the temperature stable CTNA sample at ambient conditions using Station 2.3 (Daresbury Laboratories, England). Structural characteristics were obtained from the refinement analysis. The overall lattice framework is a distorted perovskite-type structure (orthorhombic) described by the space group, *Pbnm*. The deviation from the cubic perovskite, which occurs in the structure, can be considered in terms of orthorhombic $a^-a^-c^+$ tilt system in association with displacement of the A-site cations of the perovskite structure.

References

1. Cava, R. J., Dielectric materials for applications in microwave communications. *J. Mater. Chem.*, 2001, **11**, 54–62.
2. Ubic, R., Reaney, I. M. and Lee, W. H., Microwave dielectric solid-solution phase in system BaO-Ln_2O_3-TiO_2 (Ln = lanthanide cation). *International Materials Reviews*, 1998, **43**(5), 205–219.
3. Ezaki, K., Baba, Y., Takahashi, H., Shibata, K. and Nakano, S., Microwave dielectric properties of CaO-Li_2O_3-Ln_2O_3-TiO_2 ceramics. *Jpn. J. Appl. Phys.*, 1993, **32**, 4319–4322.
4. Janèar, B., Suvorov, D. and Valant, M., Microwave dielectric properties of $CaTiO_3$-$NdAlO_3$ ceramics. *J. Mat. Sci. Lett.*, 2001, **20**, 71–72.
5. Ikoma, K.O., Suita, Y.Y and Toyonaka, K.K., *Dielectric Ceramic Composition and Dielectric Resonators*. United States Patent 5470808, 28 November 1995.
6. Wise, P. L., Reaney, I. M., Lee, W. E., Price, T. J., Iddles, D. M. and Cannell, D. S., Structure-microwave property relations in $(Sr_xCa_{(1-x)})_{n+1}Ti_nO_{3n+1}$. *J. Eur. Ceram. Soc.*, 2001, **21**, 1723–1726.
7. Kim, M.-H., Woo, C.-S., Nahm, S., Choi, C.-H., Lee, H.-J. and Park, H.-M., Crsytal structure and microwave dielectric properties of *(1-x)*$NdAlO_3$-*x*$CaTiO_3$ ceramics. *Mater. Res. Bull.*, 2002, **37**, 605–615.
8. Suvorov, D., Valant, M., Jancar, B. and Skapin, S. D., $CaTiO_3$-based ceramics: Microstructural development and dielectric properties. *Acta Chim. Slov.*, 2001, **48**, 87–99.
9. Kim, M.-H., Nahm, S., Choi, C.-H., Lee, H.-J. and Park, H.-M., Dielectric properties of (1-x)$NdGaO_3$-*x*$CaTiO_3$ solid solution at microwave frequencies. *Jpn. J. Appl. Phys.*, 2002, **41**, 717–721.
10. Huang, C.-L., Chen, H.-L. and Wu, C.-C., Improved high Q value of $CaTiO_3$–$Ca(Mg_{1/3}Nb_{2/3})O_3$ solid solution with near zero temperature coefficient of resonant frequency. *Mater. Res. Bull.*, 2001, **36**, 1645–1652.
11. Levin, I., Chan, J. Y., Maslar, J. E., Vanderah, T. A. and Bell, S. M., Phase transitions and microwave dielectric properties in the perovskite-like $Ca(Al_{0.5}Nb_{0.5})O_3$–$CaTiO_3$ system. *J. Appl. Phys.*, 2001, **90**(2), 904–914.
12. Cho, S.-Y., Youn, H.-J., Lee, H.-J. and Hong, K. S., Contribution of structure to temperature dependence of resonant frequency in the (1-x)$La(Zn_{1/2}Ti_{1/2})O_3$.x$ATiO_3$ (A = Ca, Sr) system. *J. Am. Ceram. Soc.*, 2001, **84**(4), 753–758.
13. Avdeev, M., Seabra, M. P. and Ferriera, V. M., Structure evolution in $La(Mg_{0.5}Ti_{0.5})O_3$-$SrTiO_3$ system. *Mater. Res. Bull.*, 2002, **37**, 1459–1468.
14. Okawa, Y., *Dielectric ceramic composition, preparation method thereof and dielectric resonator*. United States Patent 6143680, 7 Nov. 2000.
15. Meden, A. and Ceh, M., Rietveld refinement of $Ca_{0.54}La_{0.46}Mg_{0.23}Ti_{0.77}O_3$—a promising new microwave ceramic. *Mat. Sci. Forum.*, 2000, **321–324**, 988–993.
16. Sasaki, S., Prewitt, C. T., Bass, J. D. and Schulze, W. A., Orthorhombic perovskite $CaTiO_3$ and $CdTiO_3$: structure and space group. *Acta Cryst.*, 1987, **C43**, 1668–1674.
17. Cho, S.-Y., Kim, I.-T. and Hong, K. S., Microwave dielectric properties and applications of rare-earth aluminates. *J. Mat. Res.*, 1999, **14**(1), 114–119.
18. Tang, C. C., Roberts, M. A., Azough, F., Leach, C. and Freer, R., Synchrotron x-ray diffraction study of $Ba_{4.5}Nd_{0.9}Ti_{18}O_{54}$ microwave dielectric ceramics at 10-295 K. *J. Mat. Res.*, 2002, **17**, 675–682.
19. Collins, S. P., Cernik, R. J., Pattison, P., Bell, A. T. M. and

Fitch, A. N., A two-circle powder diffractometer for synchrotron radiation on Station 2.3 at the SRS. *Rev. Sci. Instrum*., 1992, **63**, 1013–1014.

20. Laundy, D., Tang, C, Roberts, M., Miller, M., Thompson, S. and Bushnell-Wye, G., Software for automation calibration of synchrotron powder diffractometer. *J. Synchrotron Rad*., 2003, **10**, 183–186.
21. Rietveld, H. M., A profile refinement method for nuclear and magnetic structures. *J. Appl. Cryst*., 1969, **2**, 65–71.
22. Glazer, A. M., Simple ways of determining Perovskite structures. *Acta Cryst*., 1976, **A31**, 756–762.
23. Thomas, N. W., A framework for analysing relationships between chemical composition and crystal structure in metal oxides. *Acta Cryst*., 1991, **B47**, 180–191.